12th IEA Heat Pump Conference 2017

Analysis on shock waves characteristics of driving flow inside the ejector

CHEN Zuozhou[a], DANG Chaobin[a,*], HIHARA Eiji[a]

[a] Institute of Environmental Studies, Graduate School of Frontier Sciences, The University of Tokyo, 5-1-5 Kashiwanoha, Kashiwa-shi, Chiba 277-8563, Japan

Abstract

In this research, experimental and numerical investigations have been conducted on the driving flow Mach wave inside ejectors under off-design operation conditions. Numerical investigation has been conducted by the method of characteristics, and a simulation model was established to obtain the driving flow development from the nozzle exit. The influence of Mach waves from the nozzle exit was taken into consideration in the simulation model. Visualization experiment has also been conducted to validate the simulation results in the current research. Through this investigation, the influence of Mach wave on the driving flow boundary development is discussed. The expansion wave from the nozzle exit increases the driving flow regime in the under-expanded condition, which has negative impact on ejector performance. The results show that the Mach wave should be considered when the ejector is operated under off-design working conditions, and appropriate nozzle structure design was able to restrain the effect of the expansion wave, which improves ejector performance.

Keywords: ejector, Schlieren photography, method of characteristics, numerical simulation, visualization

1. Introduction

Large-scale applications for air conditioning and refrigeration systems consume huge amounts of energy and cause environmental problems. Efforts to reduce the level of energy consumption in these applications have led to renewed interest in heat recovery systems. Heat recovery refrigeration systems are an alternative to vapor-compression refrigeration systems. In these systems, low-grade heat such as solar energy or exhausted heat can be utilized as the driving energy. The ejection refrigeration cycle is one example of such heat recovery systems with simple-structure, high reliability, and low-cost. In recent years, related publications on ejectors or ejection refrigeration cycles has grown rapidly [1]. Fig.1 shows the structure of an ejector. The ejector comprises of a motive nozzle, a suction chamber, a mixing section, and a diffuser. High pressure refrigerant, hereafter driving flow, is accelerated through the motive nozzle and converted into high velocity flow with low pressure. The suction flow is entrained into the ejector from the suction flow inlet. On the shear layer of the driving flow boundary, part of the kinetic energy from the driving flow is transferred to the suction flow. The two flows will finally mix in the mixing section and jet outward from the diffuser. The performance of the ejector is described by the parameter *ER* (the Entrainment Ratio) and *PR* (the Pressure Ratio) as shown by Eq. (1), (2).

* Corresponding author. Tel.: +81-04-7136-6467
E-mail address: dangcb@k.u-tokyo.ac.jp.

$$ER = \dot{m}_{\text{suctionflow}} / \dot{m}_{\text{drivingflow}} \quad (1)$$

$$PR = P_{\text{b}} / P_{\text{s,0}} \quad (2)$$

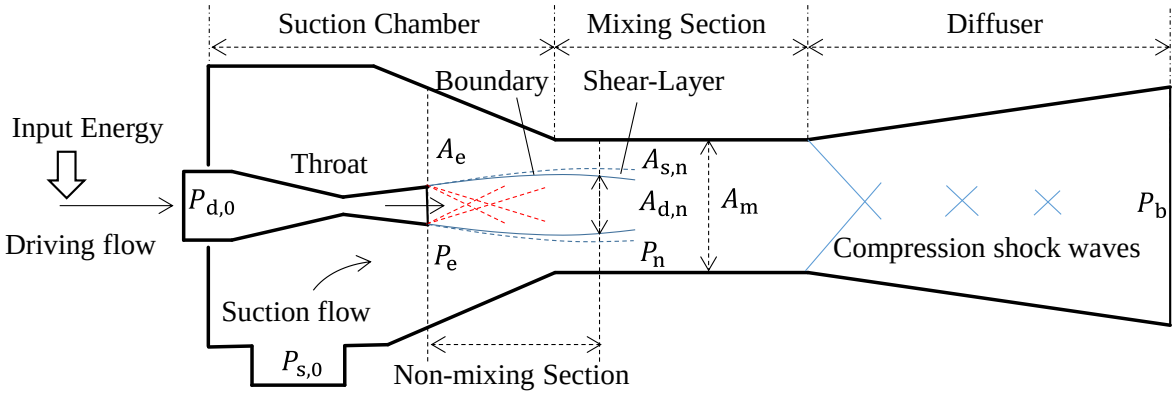

Fig. 1 Schematic of the ejector and the Mach wave positions

As the key parameter in the ejector performance evaluation, ER is obtained by predicting the effective area of the suction flow. The theory of an effective area is proposed by Huang et al. [2], in which the driving and suction flow are considered flowing separately and start to mix from the effective area. Thus the suction flow rate is defined by the effective area and the velocity of the suction flow on the cross-section. Since the ejector structure is fixed, the relationship of the flow areas could be obtained by predicting the flow area of the driving flow as shown in Eq. (3), and the calculation process of ER was introduced in the one-dimensional model developed by Huang et al [3].

$$A_{\text{s,n}} + A_{\text{d,n}} = A_{\text{m}} \quad (3)$$

In applications such as waste heat utilization, a relatively stable heat source temperature could be obtained therefore it is able to design an ejector with ideal driving flow expansion. Thus the driving flow cross-section area could be obtained by assuming that the driving flow undergoes isentropic expansion from the nozzle exit as shown in Eq. (4) and (5).

$$\frac{P_n}{P_e} = \frac{(1+M_{\text{d,n}}^2(\gamma-1)/2)^{\gamma/(\gamma-1)}}{(1+M_{\text{e}}^2(\gamma-1)/2)^{\gamma/(\gamma-1)}} \quad (4)$$

$$\frac{A_{\text{d,n}}}{A_{\text{e}}} = \frac{(1/M_{\text{d,n}})\left[2/(\gamma+1)(1+M_{\text{d,n}}^2(\gamma-1)/2)\right]^{(\gamma+1)/(2(\gamma-1))}}{(1/M_{\text{e}})\left[2/(\gamma+1)(1+M_{\text{e}}^2(\gamma-1)/2)\right]^{(\gamma+1)/(2(\gamma-1))}} \quad (5)$$

Yet, in other cases, especially for solar energy utilization, due to the change in heat source temperature, the driving flow will be in either the over-expanded or under-expanded condition. Under off-design conditions, Mach waves may develop and influence the ejector performance. Shockwaves in the over-expanded condition cause irreversible energy loss in the driving flow. On the other hand, expansion waves in the under-expanded condition creates radial velocity components in the driving flow, which will reduce the flow area of the suction flow regime. To employ ejection cycles in solar energy utilization, the influence of Mach wave should be considered. However, there have not been many studies aimed toward the occurrence of Mach waves and its influence on ejector performance.

In this research, the Mach wave in the gas-ejector at the off-design working condition is discussed. The influence of Mach wave on the driving flow expansion, as well as the ejector performance, is investigated numerically and experimentally. A numerical approach using the method of characteristics model is adopted to predict the driving flow expansion inside an ejector. The simulation results are further validated by visualization experiments

conducted using the Schlieren photography method. The research reveals the influence of Mach wave on the ejector performance, which is significant for the application of solar-driven ejection–refrigeration cycles.

2. Simulation Methodology

As shown in Fig.2, the driving flow field is divided into three parts, marked as Ⅰ, Ⅱ, and Ⅲ. The three parts represent the flow field before, inside, and after the expansion fan. In the under-expanded condition, an expansion fan is formed by a group of expansion waves propagating from the nozzle exit rim. The expansion fan depressurizes the driving flow pressure to suction flow pressure at the nozzle exit, and gives an out-turning flow angle to the driving flow. The driving flow pressure will further decrease in flow regime Ⅲ because of this flowing angle. In regime Ⅲ, when the driving flow pressure is smaller than the environmental pressure, a shockwave will originate from the boundary to correct the driving flow pressure and flow direction. In summary, the Mach wave is the propagation of physical disturbances caused by a pressure difference, and the driving flow regime is influenced by both expansion waves and shockwaves. The method introduced by M.J. Zucrow and J.D. Hoffman is adopted in this study [4] and several assumptions are clarified:

1. The outflow from the nozzle is parallel with unified velocity.
2. The flow field is axisymmetric to the x-axis.
3. The flow is supersonic throughout the driving flow regime.
4. Friction between driving flow and suction flow is neglected.
5. The calculation proceeds under an ideal gas assumption with constant C_p and γ.
6. The suction flow is considered as one-dimensional flow, accelerated in a converging tunnel formed by the driving flow boundary and the ejector wall, the suction flow pressure along the tunnel functions as the environment pressure for the driving flow.
7. The driving flow pressure is equal to the suction flow pressure on the boundary.

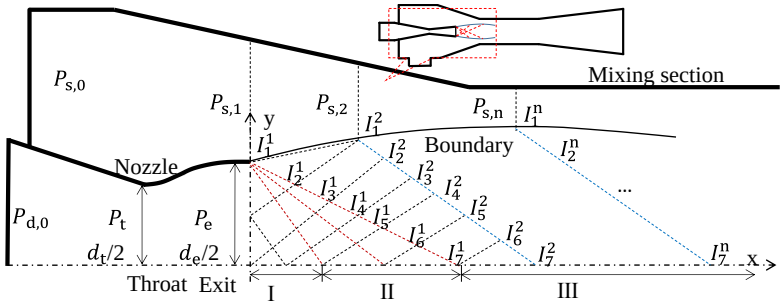

Fig.2 Flow fields presented by the method of characteristics model in the under-expanded condition

To describe the driving flow, the governing equations for a two-dimensional, irrotational, inviscid flow are presented as shown in Eq. (6). A grid is constructed inside the driving flow, the points are intersections of the characteristics curves. Property of each point downstream from the nozzle exit could be obtained by two other points upstream as shown in Fig. 2.

$$\begin{pmatrix} u^2-a^2 & 2uv & v^2-a^2 & 0 \\ 0 & 1 & -1 & 0 \\ \mathrm{d}x & \mathrm{d}y & 0 & 0 \\ 0 & 0 & \mathrm{d}x & \mathrm{d}y \end{pmatrix} \begin{pmatrix} u_x \\ u_y \\ v_x \\ v_y \end{pmatrix} = \begin{pmatrix} \delta a^2 v / y \\ 0 \\ \mathrm{d}u \\ \mathrm{d}v \end{pmatrix} \tag{6}$$

Since u_x is discontinuous but not infinite along the characteristic curve, it is obtained from Eq. (6) by the Cramer's rule and further presented as show in Eq. (7). The positions of the points linked by characteristics curves could further be expressed by Eq. (11).

$$(u^2-a^2)\mathrm{d}u_{\pm} + \left[2uv-(u^2-a^2)\lambda_{\pm}\right]\mathrm{d}v_{\pm} - (\delta\frac{a^2 v}{y})\mathrm{d}x_{\pm} = 0 \tag{7}$$

Where

$$\left(\frac{\mathrm{dy}}{\mathrm{dx}}\right)_{\pm} = \lambda_{\pm} = \tan(\theta \pm \beta) \tag{8}$$

$$\theta = \arctan\left(\frac{v}{u}\right) \tag{9}$$

$$\beta = \pm\arctan\left(\frac{1}{M}\right) \tag{10}$$

$$y_c - \lambda_{\pm} x_c = y_1 - \lambda_{\pm} x_1 \tag{11}$$

Giving the boundary condition for the driving flow, an iteration methodology could be adopted from Eq. (7)-(11) to obtain the driving flow boundary development from the nozzle exit to downstream inside the ejector. Mach wave angle from the nozzle exit could be expressed by Eq. (12).

$$\sigma = -\sqrt{b}\arctan\sqrt{\frac{M^2-1}{b}} + \arctan\sqrt{M^2-1} + \sigma_0 \tag{12}$$

$$b = \sqrt{\frac{\gamma+1}{\gamma-1}}$$

On the other hand, the suction flow is considered accelerating inside a converging tunnel formed by the driving flow and ejector wall.

3. Schlieren Photography System

Fig. 3 shows a Schlieren experimental setup constructed to obtain images of flow inside of the ejector. Light originates from an LED light source, and a point light source is formed after light passes through a spatial filter. A convex is placed to produce a parallel light beam that passes through the ejector. The density discontinuities inside of the ejector caused by the Mach waves or the jet boundary cause the refraction of part of the light. When another convex lens is placed after the ejector to focus the light, the refracted light will be focused at different locations. A knife-edge is employed to block the refracted light. A high-speed camera is used to capture the Schlieren photos. In Schlieren photos, places where density discontinuity occurs are illustrated by different illuminance compared to the rest of the parts. On the ejector side, a nitrogen gas tank is used as the gas supply for both the driving and suction flow. The working condition is controlled by three regulators placed on the ejector inlets and outlet. In addition, pressure sensors are placed at the inlets and outlet of the ejector. A volumatic flow rate meter is used to measure the suction flow rate, while the driving flow rate is calculated by the measured inlet pressure and the nozzle throat diameter.

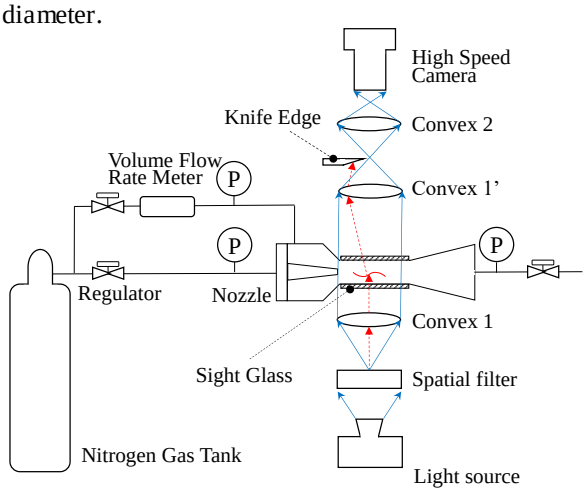

Fig. 3 Schematic of the Schlieren System

A transparent mixing section was manufactured by a 3D printer with a rectangular mixing section. The width and length of the mixing section are 4.60 mm and 3.50 mm. A subsonic nozzle and a convergent-divergent supersonic (CD) nozzle are adopted in the experiment. The subsonic nozzle has a converging duct with an outlet diameter of 1.30 mm. The CD nozzle has a throat diameter of 1.30 mm and an outlet diameter of 1.36 mm. It has an exit-to-throat area ratio of 1.094. The area from the nozzle exit is observed during the experiment.

4. Results and Discussion

4.1. Validation of the MOC simulation results

Fig. 4 shows the driving flow expansion when a CD nozzle is employed in the ejector. The driving flow pressure is adjusted from 400 kPa to 600 kPa, and the suction flow pressure is adjusted from 80 kPa to 90 kPa. Information including the driving flow boundary and the Mach wave are highlighted in the photos. In the first Mach disk, the maximum diameter of the driving flow (d_{max}) and its distance from the nozzle exit (L_{max}) are considered as the criteria for the driving flow expansion.

Fig. 5 shows the simulation results validation, it could be observed that the simulation results agree well with the measured values from the Schlieren images. Also, d_{max} and L_{max} increase as the pressure difference between the driving and suction flow increase at the nozzle exit.

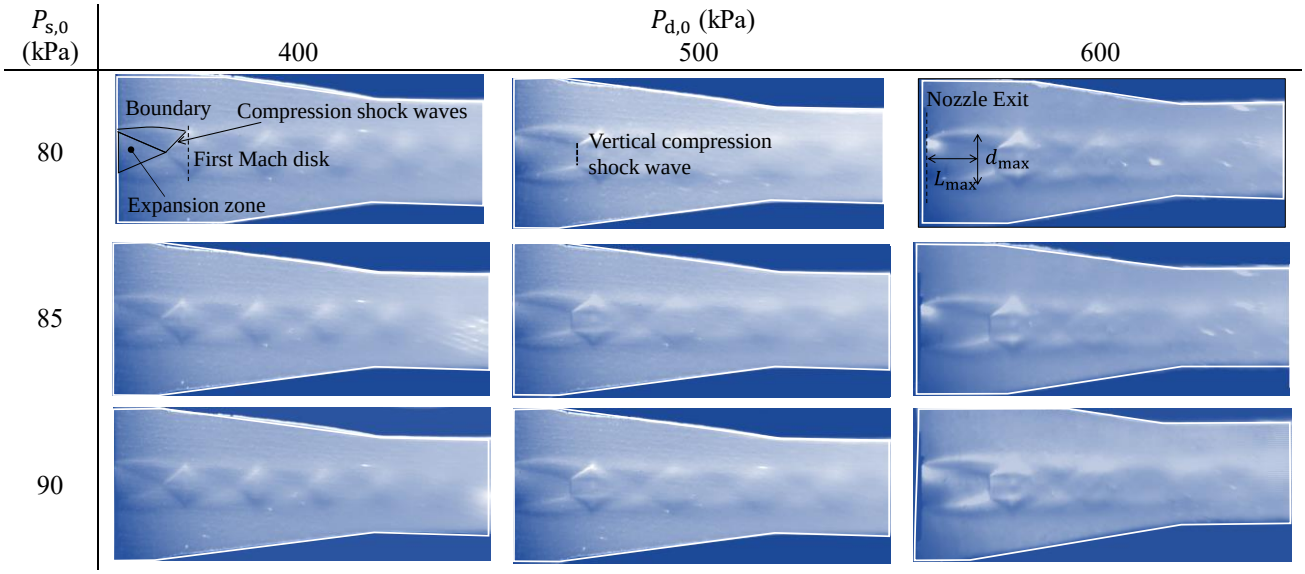

Fig. 4 Schlieren pictures under various driving and suction pressures

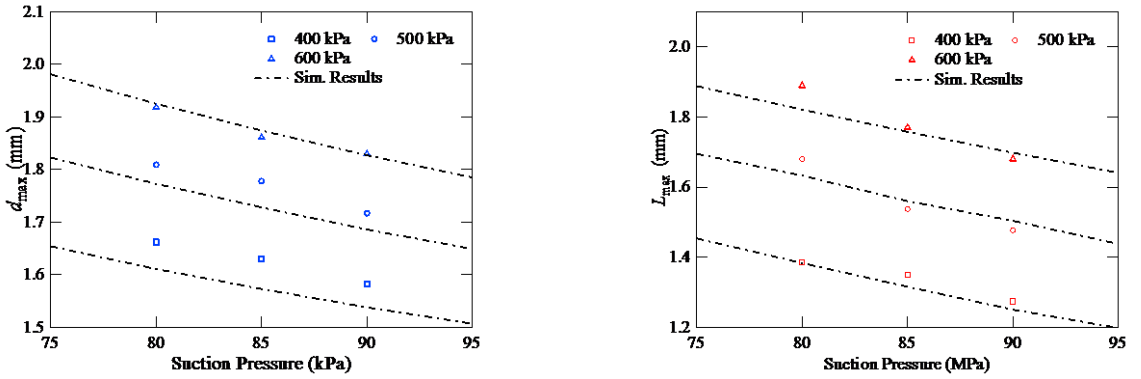

(a) Maximum driving flow diameter (b) Distance of the d_{max} surface from the nozzle exit

Fig. 5 Comparison between the MOC simulation results and the measured dimensions from the Schlieren Photos

4.2. Influence of nozzle structure on the driving flow expansion

Table 1 Nozzle configurations

	Converging-diverging nozzle	Subsonic nozzle
Throat diameter	1.30 mm	1.30 mm
Nozzle exit diameter	1.40 mm	1.30 mm

Two nozzles with different configuration are adopted to discuss the influence of nozzle structure on the driving flow expansion, the dimensions are presented in Table 1. A subsonic has a converging duct, while a converging-diverging nozzle has a diverging duct after the nozzle throat. Fig.6 shows an example of visualization results obtained at driving flow pressure of 500 kPa and suction flow pressure of 80 kPa for a CD nozzle and a subsonic nozzle. It could be observed that for both nozzles, the driving flow is in under-expanded condition. The first Mach cell from the subsonic nozzle is shorter and wider than the Mach cell from the supersonic nozzle. Extra expansion occurs from the subsonic nozzle exit, which is caused by larger pressure difference between the driving and suction flow. The extra expansion will have negative influence on the ejector performance when the operating condition as well as the ejector structure are kept constant. The *ER* comparison is presented in Fig. 7. The

experiment as well as the simulation results reveals the influence of shockwave characteristics on the ejector performance. In the perspective of flow analysis, overly expanded driving flow occurred owing to the inappropriate design of the nozzle configuration. The extra expansion of the driving flow will block part of the suction flow region in the mixing suction, which further yields performance decrease. On the other hand, according to the observation of the Schlieren images, reflected shockwave also occurs when expansion occurs from the nozzle exit, in severe cases, normal shock occurs which directly convert the supersonic flow into subsonic. The irreversible energy loss caused by shockwave is considered as another factors that has negative influence on the ejector performance.

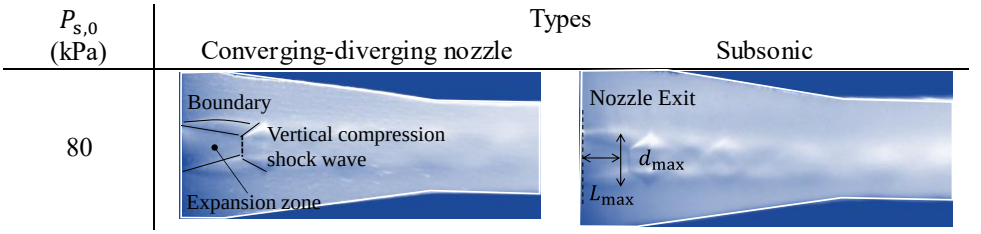

Fig. 6 Comparison between the converging-diverging nozzle and the subsonic nozzle

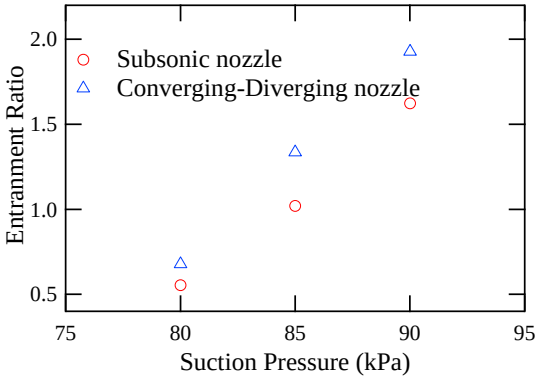

Fig.7 Entrainment Ration comparison

5. Conclusion

In this research, experimental and numerical investigations on driving flow inside the ejector were conducted, and the main conclusions are listed as follows:

1. The numerical simulation results were validated by visualization experiments conducted using the Schlieren optical system. The results show good agreement between the MOC simulation results and the measured values from the experiment.
2. The values for d_{max} and L_{max} are affected by the nozzle structure. The expansion waves from the nozzle exit strengthen the driving flow expansion, which creates a negative effect on ejector

performance. However, with an appropriate nozzle design, the performance of the ejector can be enhanced.

3. Under the off-design condition, $d_{\max}$ deviates from the predicted value according to the isentropic expansion equations. It is necessary to consider the influence of Mach wave on the ejector performance when an ejector is applied in a refrigeration system with an unstable heat source.

References

[1] S. Elbel, N. Lawrence, Review of recent developments in advanced ejector technology, International Journal of Refrigeration 2016; **62**: 1-18.
[2] B.J. Huang, W.Z. Ton, C.C. Wu, *et al*. Performance test of solar-assisted ejector cooling system, International Journal of Refrigeration 2014; **39**: 172-185.
[3] B.J. Huang, J.M. Chang, C.P. Wang, V.A. Petrenko, A 1-D analysis of ejector performance, International Journal of Refrigeration; 1999, 22 (1999) 354-364.
[4] M.J. Zucrow, J.D. Hoffman, Gas Dynamics. John Wiley & Sons, New York; 1976.